

# Whole-body, real-time preclinical imaging of quantum dot fluorescence with time-gated detection

Andrzej May,<sup>a</sup> Srabani Bhaumik,<sup>a</sup> Sanjiv S. Gambhir,<sup>b</sup> Chun Zhan,<sup>a</sup> and Siavash Yazdanfar<sup>a,\*</sup>

<sup>a</sup>GE Global Research, 1 Research Circle, Niskayuna, New York 12309

<sup>b</sup>Stanford University, Department of Radiology, Molecular Imaging Program, and Department of Bioengineering, Bio-X Program, 318 Campus Drive, Palo Alto, California 94305

**Abstract.** We describe a wide-field preclinical imaging system optimized for time-gated detection of quantum dot fluorescence emission. As compared to continuous wave measurements, image contrast was substantially improved by suppression of short-lifetime background autofluorescence. Real-time (8 frames/s) biological imaging of subcutaneous quantum dot injections is demonstrated simultaneously in multiple living mice. © 2009 Society of Photo-Optical Instrumentation Engineers. [DOI: 10.1117/1.3269675]

Keywords: fluorescence lifetime; colloidal quantum dots (QDs); near-infrared (NIR) imaging.

Paper 09368LR received Aug. 18, 2009; revised manuscript received Sep. 26, 2009; accepted for publication Oct. 9, 2009; published online Dec. 7, 2009.

Colloidal semiconductor quantum dots (QDs) are fluorescent nanoparticles used for imaging of biological particles over multiple physical scales, from the molecular<sup>1</sup> up to the organ level.<sup>2</sup> QDs feature favorable photophysical properties for biological imaging, such as high photostability, a broad excitation spectrum, and a fluorescence emission spectrum that is both narrow and tunable by size and material composition.<sup>3</sup> Additionally, the relaxation dynamics of QDs have been rigorously explored,<sup>4–6</sup> demonstrating fluorescence emission lifetimes ( $> 10$  ns) that are measurably longer than that of organic fluorophores and background autofluorescence ( $\sim 0.1$  to 5 ns). In the presence of background, the long QD lifetimes allow for improved selectivity via time-gated detection, a technique that has been exploited primarily for imaging QDs in cells or in solution.<sup>7–10</sup> In particular, the long fluorescence lifetime may be harnessed for *in vivo* small animal imaging,<sup>11</sup> where autofluorescence is most prominent. Suppression of autofluorescence background may increase sensitivity and allow for high-throughput preclinical imaging of QDs. In this letter, we develop an imaging instrument optimized for time-gated QD imaging of multiple small animals.

The desired features of such an instrument include real-time imaging and wide-field illumination and detection for high-throughput imaging of one or more animals simulta-

neously. Time-gated detection may be employed to suppress background autofluorescence and maximize QD contrast. Furthermore, the system should be designed for imaging of red to near-infrared (NIR) QDs, owing to the reduced scattering and autofluorescence in this spectral range.<sup>12</sup> To meet these requirements, a wide-field ( $\sim 100$  cm<sup>2</sup>) NIR gated detection system (Fig. 1) was built to evaluate gated imaging approaches for high-speed imaging of longer fluorescence decay time (10 to 100 ns) molecular imaging agents *in vivo*. The imaging system consisted of a pulsed high-power 630-nm LED excitation array and a gated intensified CCD camera for fluorescence detection (details in figure caption). The excitation light was bandpass filtered with interference filters at  $615 \pm 20$  nm to block excitation light that overlapped with the QD emission peak. Similarly, the collected light was filtered with an interference filter at  $710 \pm 25$  nm on the lens of the image intensifier to pass only the QD emission wavelengths.

Two independent RF power amplifiers driven by phase-locked arbitrary wave form generators provided control wave forms for the intensifier gate and LED excitation. The excitation and detection gating timing sequences used in this study are shown in Fig. 1(b). Excitation light was pulsed at 2-MHz pulse repetition frequency with high electrical peak power (10 W) and low duty cycle (3%). Images that were equivalent to conventional fluorescence imaging, which normally uses continuous-wave (CW) excitation light, were synthesized on our system by overlapping the excitation pulse and intensifier detection window times during the image exposure. Alternatively, time-gated images were obtained by inserting a delay between the end of the excitation pulse and start of the detection window. The molecular imaging agent used in this study, QD705 (Invitrogen, Q21061MP), had a relatively long fluorescence lifetime ( $> 20$  ns)<sup>13</sup> compared to most tissue autofluorescence components ( $\sim 0.1$  to 5 ns).<sup>12</sup> Thus, delaying the detection window increased rejection of scattered excitation light and fast-decay fluorescent emissions known to comprise a significant proportion of tissue autofluorescence. This gating scheme enhanced the contrast of the QD against autofluorescence background and backscattered excitation light.

During the experiment, the exposure time and imaging lens aperture were manually adjusted to utilize the dynamic range of the detection system without saturating the CCD camera. The optimal gate delay for contrast enhancement of QD705 was selected qualitatively and empirically during real-time imaging by visual examination of the image contrast obtained with different gate delays, on the order of  $\sim 50$  ns, leading to attenuation of background autofluorescence. Exposure times ranged from 0.125 s for conventional (CW) fluorescence imaging up to 5 s for time-gated imaging of the lowest QD concentrations (0.25 nM). Longer exposure times were typically used for the QD-gated imaging because the emission intensity is exponentially lower with longer gating delays.

A stock solution of nontargeted QD705 was serially diluted with phosphate buffered saline (PBS) solution to concentrations between 0.06 and 10.0 nM. QD concentrations were measured with absorption spectrometry at 405 nm (Perkin Elmer Lambda 20) within 24 h of the imaging study. The solutions were pipetted into a well plate in order to measure

\*Address all correspondence to: Siavash Yazdanfar, GE Global Research, KW C287, 1 Research Circle, Niskayuna, NY 12309. Tel: 518-387-5000; Fax: 518-387-7021; E-mail: siavash.yazdanfar@research.ge.com

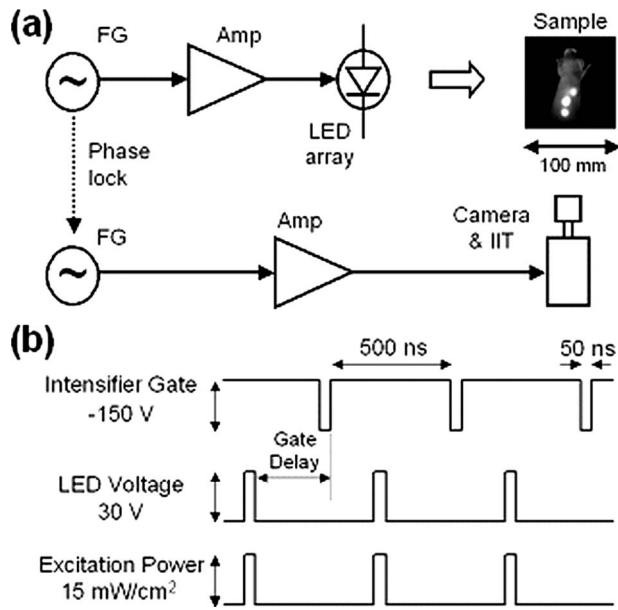


**Fig. 1** (a) Schematic diagram of wide-field time-gated imaging system. Phase-locked function generators (FG, Agilent 33250) are amplified (ENI 350L RF power amp) to provide the drive voltage for the light source (Luxeon ND93LXHL LED array) excitation and image intensifier tube (IIT, Hamamatsu V7090U-71-G130RG/NG) photocathode modulation. The IIT phosphor is imaged by a CCD camera (Basler A312f) operating at 8 fps. (b) Timing diagram for excitation and detection gating.

the instrument linearity and sensitivity in the absence of background fluorescence, as shown in Fig. 2. The lowest concentration (0.06 nM) was easily discernible from the instrument noise floor, and the signal was linear over the response of the 8-bit camera.

*In vivo* imaging was performed in accordance with a protocol approved by the Institutional Animal Care and Use Committee at GE Global Research. QD-in-PBS solutions were diluted 1:1 by volume with Matrigel (BD Biosciences) to 50  $\mu$ L immediately prior to subcutaneous injection in multiple separate locations along the back of three anesthetized nude mice (Charles River Laboratories). The Matrigel is used to keep the QDs relatively well contained at the site of injection *in vivo*. The CW image of QD-Matrigel injections in 10 locations along the backs of three nude mice [Fig. 3(a)] detected fluorescent inclusions from the injection sites where relatively higher concentrations of contrast agent (on the order of 2.5 nM) were present. However, lower concentration injections were not discernible from the background autofluorescence

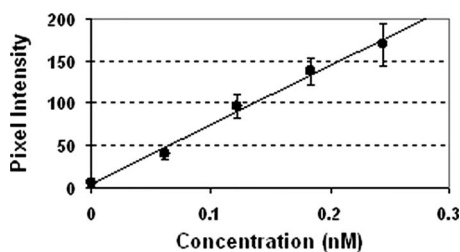


**Fig. 2** Image pixel intensity (8-bit) indicating a linear signal response and sensitivity below 0.1 nM, measured *in vitro*.

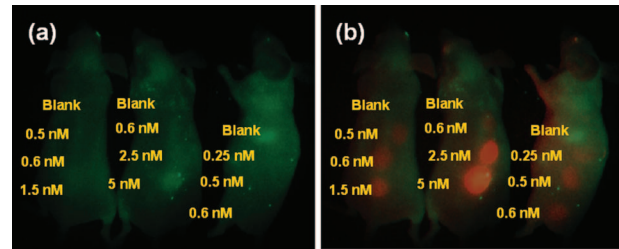


**Fig. 3** Wide-field fluorescent imaging of subcutaneous QD injections in nude mice. (a) Image obtained with CW illumination shows poor discrimination of QDs. (b) Composite image of time-gated (red) and CW (green) detection allows for high-contrast measurement of QDs.

cence of the mouse skin using CW fluorescence imaging. In comparison, data obtained with time-gated imaging on the same mice [Fig. 3(b)] had greatly improved contrast of the QD inclusion relative to background, allowing detection of QD concentrations down to 0.25 nM. Total fluorescence intensity was decreased substantially with gating, requiring 5 to 10 $\times$  longer exposure times to obtain image intensities equivalent to CW images.

Overall, *in vivo* image contrast (defined as signal in a region of interest divided by autofluorescence background) increased by a factor of 3 to 10 through time-gated detection. This improved the detection limit by  $\sim 10\times$ , from 2.5 nM to 0.25 nM of QD705 in 50- $\mu$ L injections [Fig. 4(a)]. However, considering that the gate delays were adjusted empirically to maximize image contrast, measurement of absolute intensities does not directly correlate to QD concentrations. Histograms of the measured background autofluorescence [Fig. 4(b)] indicate that gating reduced the background intensity while increasing its uniformity. Reduced background intensity (i.e., histogram mean, lowered from 33.0 to 7.46) improved visualization of the QD inclusions. Contrast enhancement observed with gated imaging was also due in part to a significant increase of the background autofluorescence uniformity (i.e., histogram width, lowered from 13.6 to 3.54) in the regions of the mice where QDs were absent. This increased uniformity in the gated background markedly enhanced visualization of QD inclusion sites with little difference in the absolute pixel intensities between the background and QD regions. The improved uniformity ( $\sim 4\times$ ) after time-gating may be related to the distribution of long-lifetime versus short-lifetime endogenous fluorophores *in vivo*, since the shorter-lifetime fluorophores are more abundant and thus generate a greater intensity variation. For example, the digestive system contributes substantially to short lifetime ( $< 1$  ns) background fluorescence from both endogenous sources as well as food. Given the high irradiance (up to 20 mW/cm<sup>2</sup>) at the sample, significant excitation light penetrates through the skin, resulting in a large portion of the measured emission intensity variation even though internal organs were not directly exposed during imaging.

In summary, we have demonstrated a time-gated imaging system for whole-body imaging of QDs in living animals. Lifetime-sensitive imaging offers advantages over continuous-wave (CW) imaging,<sup>11,14,15</sup> from revealing interactions of dyes with their local microenvironment to reducing background, but often requires substantially longer image acquisition times. Compared to previous studies, our system pa-

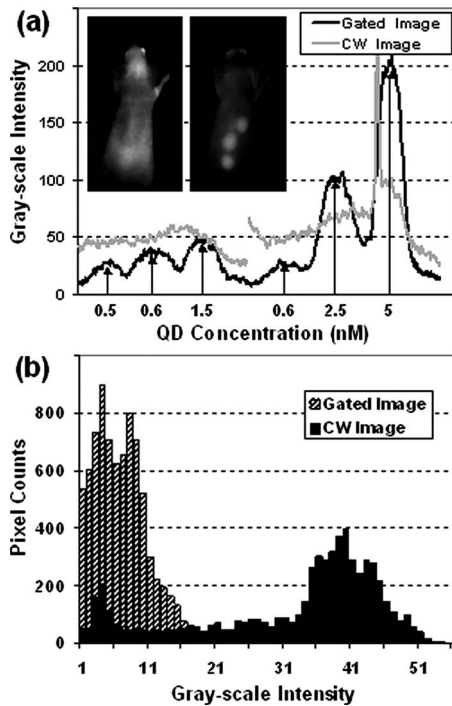


**Fig. 4** (a) Image intensity profiles, taken through the center of the QD inclusions, show substantially improved QD contrast using gated versus CW imaging. Numbers along the abscissa indicate the injected QD concentrations. Insets allow comparison of CW (left) and gated (right) images of 0.5- 1.5-nM inclusions using the same grayscale intensity. (b) Histograms of autofluorescence intensity indicate a more uniform background in time-gated imaging.

rameters were optimized for high-speed imaging of multiple mice and suppression of autofluorescence. The increase in image contrast resulting from reduced background autofluorescence enables high-sensitivity imaging of living small animals with high throughput. Time-gated imaging is especially advantageous for suppression of short-lifetime autofluorescence to enhance luminescence from longer lifetime molecular imaging agents such as QDs, porphyrins, and lanthanides.<sup>16</sup> Despite the appreciable improvement in contrast, gated imaging also suppressed a portion of the target fluorophore emission. This required the use of a more sensitive photodetector than what is typically used with conventional fluorescence imaging, as well as longer image exposures to collect sufficient light to form an image. Furthermore, additional electronic components such as a gated intensifier, RF power amplifiers, and phase-locked function generators were required for pulsed excitation and gated detection, increasing the relative cost and complexity compared to conventional fluorescence imaging. Thus, time-gated methods are not likely to replace conventional imaging of QDs, but they may serve a complementary role in specific applications where the fluorescence intensity is smaller than the background tissue autofluorescence. Additionally, by collecting images while stepping the gate delay, the fluorescence lifetime decay curve may be measured to provide biochemical information.<sup>17</sup> Time-gated imaging may be combined with multispectral detection<sup>2</sup> to allow

for discrimination of QDs along both temporal and spectral dimensions.

*Acknowledgments*

The authors acknowledge fruitful discussions with Adam de la Zerda and Dr. Bryan Ronain Smith of Stanford University. This work was supported by National Institutes of Health Grant Nos. NCI 1 U54 CA119367, NIBIB BRP 5-RO1-EBB000312, and ICMIC P50 CA114747.

*References*

1. M. Dahan, S. Lévi, C. Luccardini, P. Rostaing, B. Riveau, and A. Triller, "Diffusion dynamics of glycine receptors revealed by single-quantum dot tracking," *Science* **302**, 442–445 (2003).
2. X. H. Gao, Y. Cui, R. Levenson, L. Chung, and S. Nie, "In vivo cancer targeting and imaging with semiconductor quantum dots," *Nat. Biotechnol.* **22**, 969–976 (2004).
3. X. Michalet, F. F. Pinaud, L. A. Bentolila, J. Tsay, S. Doose, J. Li, G. Sundaresan, A. Wu, S. Gambhir, and S. Weiss, "Quantum dots for live cells, in vivo imaging, and diagnostics," *Science* **307**, 538–544 (2005).
4. G. Schlegel, J. Bohnenberger, I. Potapova, and A. Mews, "Fluorescence decay time of single semiconductor nanocrystals," *Phys. Rev. Lett.* **88**, 137401 (2002).
5. B. R. Fisher, H. Eisler, N. Stott, and M. Bawendi, "Emission intensity dependence and single-exponential behavior in single colloidal quantum dot fluorescence lifetimes," *J. Phys. Chem. B* **108**, 143–148 (2004).
6. V. Fomenko and D. Nesbitt, "Solution control of radiative and non-radiative lifetimes: a novel contribution to quantum dot blinking suppression," *Nano Lett.* **8**, 287–293 (2008).
7. A. C. Mitchell, S. Dad, and C. Morgan, "Selective detection of luminescence from semiconductor quantum dots by nanosecond time-gated imaging with a colour-masked CCD detector," *J. Microsc.* **230**, 172–176 (2008).
8. M. Dahan, T. Laurence, F. Pinaud, D. Chemla, A. Alivisatos, M. Sauer, and S. Weiss, "Time-gated biological imaging by use of colloidal quantum dots," *Opt. Lett.* **26**, 825–827 (2001).
9. H. E. Grecco, K. Lidke, R. Heintzmann, D. Lidke, C. Spagnuolo, O. Martinez, E. A. Jares-Erijman, and T. Jovin, "Ensemble and single particle photophysical properties (two-photon excitation, anisotropy, FRET, lifetime, spectral conversion) of commercial quantum dots in solution and in live cells," *Microsc. Res. Tech.* **65**, 169–179 (2004).
10. G. Giraud, H. Schulze, T. Bachmann, C. Campbell, A. Mount, P. Ghazal, M. Khondoker, A. Ross, S. Ember, I. Ciani, C. Tlili, A. Walton, J. Terry, and J. Crain, "Fluorescence lifetime imaging of quantum dot labeled DNA microarrays," *Int. J. Mol. Sci.* **10**, 1930–1941 (2009).
11. D. J. Hall, U. Sunar, S. Farshchi-Heydari, and S. Han, "In vivo simultaneous monitoring of two fluorophores with lifetime contrast using a full-field time domain system," *Appl. Opt.* **48**, D74–D78 (2009).
12. R. Richards-Kortum and E. Sevick-Muraca, "Quantitative optical spectroscopy for tissue diagnosis," *Annu. Rev. Phys. Chem.* **47**, 555–606 (1996).
13. M. D. Holton, O. Silvestre, R. Errington, P. Smith, D. Matthews, P. Rees, and H. Summers, "Stroboscopic fluorescence lifetime imaging," *Opt. Express* **17**, 5205–5216 (2009).
14. S. Keren, O. Gheysens, C. Levin, and S. Gambhir, "A comparison between a time domain and continuous wave small animal optical imaging system," *IEEE Trans. Med. Imaging* **27**, 58–63 (2008).
15. W. J. Akers, M. Berezin, H. Lee, and S. Achilefu, "Predicting in vivo fluorescence lifetime behavior of near-infrared fluorescent contrast agents using in vitro measurements," *J. Biomed. Opt.* **13**, 054042 (2008).
16. S. W. Botchway, M. Charnley, J. Haycock, A. Parker, D. Rochester, J. Weinstein, and J. Williams, "Time-resolved and two-photon emission imaging microscopy of live cells with inert platinum complexes," *Proc. Natl. Acad. Sci. U.S.A.* **105**, 16071–16076 (2008).
17. J. Requejo-Isidro, J. McGinty, I. Munro, D. Elson, N. Galletly, M. Lever, M. Neil, G. Stamp, P. French, P. Kellett, J. Hares, and A. Dymoke-Bradshaw, "High-speed wide-field time-gated endoscopic fluorescence-lifetime imaging," *Opt. Lett.* **29**, 2249–2251 (2004).